IGFL2-AS1-induced suppression of HIF-1α degradation promotes colorectal cancer cell proliferation by upregulating CA9

Mengdi Qin
The First Affiliated Hospital of Chongqing Medical University
Qiang Liu
The First Affiliated Hospital of Chongqing Medical University
Wei Yang
The First Affiliated Hospital of Chongqing Medical University
Qiaofeng Wang
The First Affiliated Hospital of Chongqing Medical University
Zheng Xiang (13330209937@163.com)
The First Affiliated Hospital of Chongqing Medical University

Research Article

Keywords: CA9, colorectal cancer, HIF-1α, IGFL2-AS1, proliferation

Posted Date: May 12th, 2022

DOI: https://doi.org/10.21203/rs.3.rs-1632505/v1

Abstract

Purpose: The lncRNA IGFL2-AS1 is a known cancer-promoting factor in colorectal cancer (CRC); nonetheless, the mechanism of its carcinogenic effects has not yet been elucidated. This study elaborated the role and underlying molecular mechanism of IGFL2-AS1 in promoting CRC cell proliferation.

Methods: IGLF2-AS1 expression levels in CRC tissue/normal tissue and CRC cell line/normal colon epithelial cell line were detected by quantitative real-time polymerase chain reaction. Cell Counting Kit-8, colony formation assays, and EdU assays were performed to assess the effect of IGFL2-AS1 knockdown or overexpression on the proliferative capacity of CRC cells. The expression relationship between IGFL2-AS1 and carbonic anhydrase 9 (CA9) and the CA9 expression level in CRC tissues and cells was verified by transcriptome sequencing, western blotting, and immunohistochemical staining. Treatment with MG132 and cycloheximide was utilized to explore the mechanism by which IGFL2-AS1 affects the hypoxia-inducible factor-1α (HIF-1α)/CA9 pathway. A nude mouse xenograft model was constructed to evaluate the effect of IGFL2-AS1 on CRC growth *in vivo*.

Results: We discover that IGFL2-AS1 was sharply upregulated in CRC tumor tissues and cells. IGFL2-AS1 could functionally promote CRC cell proliferation *in vitro* and accelerate CRC occurrence *in vivo*. Mechanistic studies demonstrated that IGFL2-AS1 upregulated the CA9 level by affecting the degradation pathway of HIF-1α, which elucidates its pro-proliferative effect in CRC. The lncRNA IGFL2-AS1 mediated the inhibition of HIF-1α degradation in CRC and increased CA9 expression, thereby promoting CRC progression. **Conclusion:** Our findings suggested that IGFL2-AS1 is expected to be a new promising diagnostic marker and therapeutic target for CRC.

1 Introduction

Colorectal cancer (CRC) is a lethal disease that seriously threatens human health; the incidence and mortality rates of CRC are among the top three of all malignancies worldwide and are increasing annually.[1] Despite tremendous progress in traditional treatment modalities such as modified surgery and neoadjuvant chemotherapy, the prognosis of CRC remains poor owing to high heterogeneity and recurrence rates.[2] CRC progression involves changes in colonic mucosal cells, ranging from benign adenomatous polyps to highly heterogeneous advanced invasive adenocarcinomas. The accumulation of genetic mutations and epigenetic modifications are involved in the above-mentioned multistage tumorigenesis.[3, 4] Hence, clarifying the molecular mechanism underlying CRC initiation and development may provide critical new avenues for improved diagnosis and treatment.

Currently, research on the molecular mechanism of CRC focuses more on protein-coding genes.[3] However, the development of high-throughput sequencing technology has revealed that < 2% of genes can encode proteins.[5] The advent of complete genome sequences has led to the discovery of extensive transcription of noncoding RNAs.[6] lncRNAs are RNA transcripts over 200 bp in length with little protein-coding ability.

As new players in epigenetics, lncRNAs provide irreplaceable functions in the gene regulation of CRC.[7] For example, the lncRNA ZFAS1 promotes small nucleolar RNA-mediated 2'-O-methylation through NOP58 recruitment in CRC,[8] and the lncRNA RAMS11 regulates topoisomerase IIα (TOP2α) to promote metastatic CRC progression.[9] Although the functions of a few lncRNAs in CRC have been characterized, there is still a great diversity of unknown lncRNAs that may potentially play pivotal roles in CRC.

The lncRNA IGFL2-AS1 is an antisense RNA of insulin-like growth factor-like (IGFL) family member 2, which is located on chromosome 19 and has a transcript of 1665 bp. According to previous studies, IGFL2-AS1 can promote the Wnt/β-catenin signaling pathway to activate the progression of tongue squamous cell carcinoma;[10] in breast cancer, IGFL2-AS1, as a downstream gene of KLF5, promotes IGFL1 expression.[11] IGFL2-AS1 can also act as a molecular sponge to competitively bind to miR-802 and participate in the regulation of gastric cancer.[12] A microarray analysis of 644 CRC samples from The Cancer Genome Atlas (TCGA) database (https://cancergenome.nih.gov/) showed that IGFL2-AS1 expression was significantly higher in the stem subtype than in the non-stem subtype.[13] A recent study found that IGFL2-AS1 can promote the proliferation, migration, and invasion of CRC cells *in vitro*.[14] However, the molecular mechanism by which IGFL2-AS1 exerts a tumor-promoting effect in CRC remains unclear.

Carbonic anhydrase (CA) is a large class of zinc metalloenzymes, and the transmembrane protein CA9 is one of the known tumor-associated CA isozymes. CA9 is regulated by the transcription factor hypoxia-inducible factor-1α (HIF-1α), which can regulate the pH value inside and outside of tumor cells, and indicate the progression of malignant tumors.[15–18] Previous studies have confirmed that CA9 can serve as an independent predictor for poor outcomes in CRC.[19, 20]

In this study, we aimed to explore the underlying molecular mechanisms by which IGFL2-AS1 plays a role in promoting CRC progression. Based on the basis of functional experiments and the results of transcriptome sequencing analysis, we proposed and validated the hypothesis that IGFL2-AS1 promotes CRC cell proliferation by upregulating CA9.

2 Materials And Methods

2.1 Human tissue samples

This study was conducted in accordance with the principles embodied in the Declaration of Helsinki. The experimental protocol involving human tissues for this study was approved by the Ethics Committee of the First Affiliated Hospital of Chongqing Medical University. Additionally, for this study, written informed consent was obtained from each human tissue provider. Forty pairs of CRC tumor tissue and adjacent non-tumor tissue samples were collected from patients who had undergone resection of the primary CRC at the First Affiliated Hospital of Chongqing Medical University (Chongqing, China). Cases were screened according to the following criteria: the resected specimen was confirmed to be CRC by pathological

examination, patients did not receive chemotherapy or radiotherapy preoperatively, and patients with hereditary CRC such as Lynch syndrome were excluded. After harvesting, tissue specimens were immediately frozen in liquid nitrogen and stored at -80℃ until use.

2.2 Cell lines and culture conditions

Five CRC cell lines, including SW480, SW620, Caco2, HT29, and LoVo, the human normal colon epithelial cell line NCM460, and the human embryonic kidney cell line HEK293T were purchased from the Cell Bank of the Chinese Academy of Sciences (Shanghai, China). All cells were cultured in Dulbecco's modified Eagle's medium (DMEM, Gibco, NY, USA) with 10% fetal bovine serum (FBS, Gibco, NY, USA) and 1% penicillin streptomycin solution (Beyotime, Shanghai, China. The cultural environment was a 37℃ incubator with 5% CO_2. No mycoplasma contamination was found in any of the cell lines, as indicated by mycoplasma detection kits (Lonza, Switzerland).

2.3 RNA extraction and Real-Time Quantitative Reverse Transcription PCR (qRT-PCR)

Total RNA from cells and tissues was extracted with Trizol reagent (Invitrogen, CA, USA) and stored at -80℃. RNA concentration and the optical density (OD) value were measured with the Nano-500 microspectrophotometer (Allsheng, Hangzhou, China). Next, 1 μg RNA was used to synthesize cDNA using the Prime-Script™ RT kit(Takara,Tokyo,Japan)as directed by the manufacturer's instructions. In addition, 2x SYBR Green qPCR Master Mix (Bimake, TX, USA) was employed for qPCR experiments performed in the ABI StepOne Real-time Detection System (LTC, Carlsbad, USA). There were three replicate holes for each tested sample, and relative RNA levels were compared using the comparative $2^{-\Delta\Delta CT}$ method. Glyceraldehyde 3-phosphate dehydrogenase (GAPDH) was amplified as the internal reference. The primer sequences for qRT-PCR are shown in Table S1 and were synthesized by the TsingKe Company (Chongqing, China)

2.4 Subcellular fractionation

The cytoplasmic and nuclear fractions of the HT29 and LoVo cells were isolated using the Minute™ Cytoplasmic and Nuclear Extraction Kit (Invent, Plymouth, USA) in accordance with the instruction manual. Cytoplasmic and nuclear RNA were then extracted by Trizol reagent. qRT-PCR was performed to measure the relative expression levels of cytoplasmic and nuclear specific RNAs in CRC cells. GAPDH and U6 small nuclear RNA were considered as cytoplasmic and nuclear controls, respectively.

2.5 Plasmid construction and transfection

Short hairpin RNA (shRNA) directed against human IGFL2-AS1 and HIF-1α and negative control short hairpin negative control RNA (sh-nc) were designed (the sequences are shown in Table S2) and then inserted into the lentiviral vector pGreenPuro (SBI, CA, USA) at the EcoR I/BamH I site. For the overexpression vector (oeIGFL2-AS1 and oeCA9), the full-length cDNA of IGFL2-AS1 and the cDNA sequence containing the CDS region of CA9 were synthesized, PCR-amplified by the TsingKe Company

(Chongqing, China), and ligated into the pCDH-CMVMCS-EF1-CopGFP-T2A-puro vector (SBI, CA, USA). It was verified that the nucleotide sequences were correct in all constructed vectors by sequencing.

The packaging plasmid psPAX2, envelope plasmid pMD2.G (Addgene, MA, USA), and HEK293T cells were used for lentivirus packaging. The lentiviral vector, auxiliary packaging plasmid, and Lipofectamine 2000 (Invitrogen, CA, USA) were co-transfected according to the manufacturer's instructions, and the lentiviral supernatant of the HEK293T cells was harvested 48 h later. HT29 and LoVo cells were incubated with the viral fluid containing 10 μg/mL polybrene (Solarbio, Beijing, China) for 72 h and subsequently screened with 2 mg/mL puromycin (Beyotime, Shanghai, China) for 14 days to construct stable transfection target plasmid CRC cell lines.

2.6 Cell counting kit-8 (CCK-8) assay

Cell viability was examined by the cell counting kit (CCK)-8 assay (Beyotime, Shanghai, China). HT29 and LoVo cells from the control and treatment groups in the logarithmic growth phase were inoculated into 96-well plates at a density of 2×103 cells/well, with three replicate wells for each group. After the cells became adherent (seeding for 6 h), each well was supplemented with 10 μL of CCK-8 reagent and incubated at 37℃ for another 2 h. The OD value of all cells at 450 nm was measured using a spectrophotometric plate reader (BioTek, USA). Next, CCK-8 reagent was added to the corresponding wells at 24, 48, 72, and 96 h after cell-plating, and cell viabilities were further measured according to the OD value.

2.7 5-Ethynyl-2’-deoxyuridine (EdU) incorporation assay

Cell proliferation was tested by EdU assay using an EdU Assay Kit (C0075S, Beyotime, Shanghai, China). Following the manufacturer's protocols, 2 × 105 CRC cells that were stably transfected with lentiviral vectors were seeded in 12-well plates, which were plated with cell climbing slices and cultured overnight. Then, 10 μM EdU working solution was added to the medium and incubated at 37℃ for 2 h to complete the EdU labeling. Next, cells in each group were fixed in 4% paraformaldehyde for 15 min. After the fixative was washed off with potassium buffered saline (PBS), cells were permeabilized with 0.3% Triton X-100 for 15 min. After washing, cells were incubated with the Click Reaction Cocktail configured according to the instructions away from light for 30 min. Thereafter, the nuclei were counterstained with Hoechst 33342 for 10 min while avoiding light. Finally, fluorescence images were taken by confocal laser scanning microscopy (Leica, Germany).

2.8 Colony formation assay

A total of 2 × 103 cells in the control and treatment groups were seeded in 6-well plates and cultured in complete medium at 37°C in a humidified atmosphere with 5% CO2. The cells were harvested after 14 days and fixed with 4% paraformaldehyde at room temperature for 20 min. After the fixative was washed off with PBS, 0.1% crystal violet was used to stain all cells for 15 min. The cells were washed three times again with PBS buffer, and the number of cell colonies (> 50 cells/colony) was counted using ImageJ software (NIH, MD, USA).

2.9 RNA sequencing analysis

Total RNA was extracted from the control group and IGFL2-AS1 knockdown LoVo cells using Trizol reagent. RNA samples were subjected to RNA Sequencing Analysis by Personalbio Technology Co., Ltd (Shanghai, China).

2.10 Protein extraction and Western blotting

Total proteins from cells and mice tissues were extracted by ice-cold RIPA lysis buffer (Beyotime, Shanghai, China) containing 1% phenylmethylsulfonyl fluoride (PMSF, Beyotime, Shanghai, China). The concentration of proteins was determined using the Bicinchoninic Acid Assay (BCA) Kit (Beyotime, Shanghai, China) according to the manufacturer's protocols. Then, the cell lysates were supplied with 5× loading buffer and boiled for 8 min to fully denature the proteins.

Subsequently, 30 μg of protein sample was separated by 10% sodium dodecyl sulfatepolyacrylamide gel electrophoresis (SDS-PAGE). After electrophoresis, proteins were transferred onto polyvinylidene difluoride (PVDF) membranes in a semi-wet system. Membranes were blocked with 5% skimmed milk in 1× Tris Buffered Saline with Tween (TBST) for 120 min at room temperature. After blocking, membranes were incubated with specific primary antibodies against CA9 (1:1000, ab243660, Abcam, Cambridge, UK), HIF-1α (1:2000, 66730-1 -Ig, Proteintech, Wuhan, China), and GAPDH (1:8000, 10494-1-AP, Proteintech, Wuhan, China) at 4℃ overnight (14–16 h). Next, the membranes were washed with 1× TBST three times, followed by incubation with horseradish peroxidase-labeled goat anti-rabbit (1:2000, SA00001-2, Proteintech, Wuhan, China) or goat anti-mouse secondary antibody (1:2000, Beyotime, Shanghai, China) for 90 min at room temperature, after which any residual antibody was washed away by 1× TBST. Finally, specific protein bands were detected with the enhanced chemiluminescence ECL Kit (Advansta, CA, USA) and visualized with ChampChemi imaging system (SCS, Beijing, China). All antibodies were diluted in 1x TBST containing 5% bovine serum albumin (BSA).The gray values of all protein bands were analyzed using ImageJ software.

2.11 Immunohistochemical (IHC) staining

Human CRC tissues and nude mouse tumor tissues were fixed with 4% paraformaldehyde for 24 h, embedded in paraffin, and cut into 4 μm sections. The paraffin sections were baked at 60℃ for 2 h and dewaxed in fresh xylene for 30 min. Then, the slides were hydrated with gradient alcohol, followed by boiling in a pressure cooker containing sodium citrate for 2 min to retrieve the antigens. Next, sections cooled to room temperature were incubated with an endogenous peroxidase blocking agent for 15 min and blocked with goat serum blocking solution for 30 min. The slices were incubated with specific primary antibodies against CA9 (1:2000, ab243660, Abcam, Cambridge, UK), HIF-1α (1:300, 66730-1-Ig, Proteintech, Wuhan, China) and Ki67 (1:500, ab92742, Abcam, Cambridge, UK) overnight (14–16 h) at 4℃. After washing with PBS buffer, the slices were incubated with biotin-labeled secondary antibodies for 30 min and subsequently incubated with horseradish enzyme-labeled chain avidin solution for 30

min. Finally, positive staining was visualized with brown 3,3’-diaminobenzidine tetrahydrochloride (DAB, ZSGB, Beijing, China), and counterstaining was performed with hematoxylin. The sections were mounted with 60% neutral resin. The stained sections were scanned with the Pannoramic DESK scanner (3DHISTECH, Budapest, Hungary). The images in 200× and 400× were observed and acquired with the CaseViewer 2.4 software module (3DHISTECH, Budapest, Hungary).

2.12 Xenograft mouse model

The animal experiment protocol of this study was authorized by the Animal Experiment Ethics Committee of Chongqing Medical University. Male BALB/c-nu nude mice 4–5 weeks of age were purchased from HFK Bioscience Co., Ltd. (Beijing, China). All animals were divided randomly into four groups (n = 3 mice per group) and reared under SPF-grade sterile conditions in the Laboratory Animal Center of Chongqing Medical University. Next, 1×107 LoVo cells stably transfected with sh-nc, shIGFL2-AS1#1, pCDH, and oe IGFL2-AS1 were resuspended in 100 μL of PBS solution and subcutaneously injected into the right armpit of the nude mice in each group. Tumor volumes were measured every 4 days from day 7, which was calculated as follows: volume (mm3) = 0.5 × (largest diameter) × (smallest diameter)2. On day 27, all mice were sacrificed by cervical dislocation; the tumor tissues were collected, weighed, and photographed. Proteins from tumor tissues were extracted as previously described, and IHC staining was conducted on mice tumor sections.

2.13 Statistical analysis

Statistical analysis was performed with GraphPad Prism 8 software (GraphPad software, CA, USA). All statistical differences were analyzed using the unpaired two-tailed Student's t-test, and results were presented as means ± standard deviation (SD). The differences were considered significant for p-values < 0.05. Significance is indicated as follows: *p < 0.05, **p < 0.01 and ***p < 0.001.

3 Results

3.1 IGFL2-AS1 was significantly upregulated in CRC and predominantly localized in the cytoplasm

To identify IGFL2-AS1 expression in CRC, qRT-PCR was performed to evaluate the IGFL2-AS1 levels in 40 pairs of CRC tumor and adjacent non-cancer tissues. The results revealed that IGFL2-AS1 expression was significantly higher in tumor tissues than in adjacent non-tumor tissues (Fig. 1A). In addition, based on our data analysis of 479 CRC tissues and 42 normal colon tissues downloaded from TCGA database on April 14, 2021, we found that IGFL2-AS1 was prominently upregulated in tumor tissues (Table S3). We subsequently quantified IGFL2-AS1 expression levels in the normal colon epithelial cell line NCM460 and a panel of CRC cell lines, including SW480, SW620, HT29, LoVo, and Caco2. According to the results, it

appeared to be more highly expressed in CRC cell lines than in the NCM460 cell line (Fig. 1B). We selected HT29 and LoVo cells, which expressed relatively high IGFL2-AS1 levels, for further experiments.

Next, online protein coding potential assessment software, the Coding Potential Assessment Tool (CPAT, http://lilab.research.bcm.edu/cpat/) and the Coding Potential Calculator (CPC, http://cpc.cbi.pku.edu.cn/) were used to estimate the protein-coding potential of IGFL2-AS1, and it was found that it is almost impossible for IGFL2-AS1 to encode any protein (Fig. 1C, D). Furthermore, the results of subcellular fractionation confirmed that IGFL2-AS1 was primarily located in the cytoplasm of HT29 and LoVo cells (Fig. 1E). Taken together, these data indicate that IGFL2-AS1 was generally highly expressed in CRC and had the potential to be a novel molecular target of CRC.

3.2 IGFL2-AS1 knockdown decreased CRC cell proliferation *in vitro*, whereas IGFL2-AS1 overexpression showed enhanced proliferation

Given the considerably differential IGFL2-AS1 expression in CRC, we speculated that it may play an active biological role in CRC. Therefore, we constructed CRC cell lines with stable IGFL2-AS1 knockdown. Three shRNA sequences were designed against IGFL2-AS1, and HT29 and LoVo cells were transfected with lentiviral vectors carrying shRNA and empty control sh-nc, respectively. qRT-PCR was utilized to evaluate the knockdown efficiency of these three shRNAs. It can be seen that shIGFL2-AS1#1 knockdown affected IGFL2-AS1 expression to the greatest extent (Fig. 2A). The cell viability was examined by the CCK-8 assay. The results showed that the viability of HT29 and LoVo cells was markedly reduced in the shIGFL2-AS1#1 group compared to the sh-nc group (Fig. 2B). To further clarify the effect of IGFL2-AS1 on CRC cell proliferation, we performed EdU and colony formation experiments. The results show that the deletion of IGFL2-AS1 significantly reduced the proliferation rate and colony formation capacity of HT29 and LoVo cells (Fig. 2C, D).

In addition, we transfected HT29 and LoVo cells with the overexpression vector of IGFL2-AS1 and control vector pCDH. qRT-PCR results confirmed the successful IGFL2-AS1 overexpression (Fig. 3A). Thereafter, CCK-8, EdU, and colony formation assays were used to detect the viability and proliferation of HT29 and LoVo cells. In contrast, after exogenous IGFL2-AS1 overexpression, the viability of CRC cells was considerably increased (Fig. 3B) and proliferation was enhanced (Fig. 3C, D), as compared with those of control cells. Collectively, these results suggest that IGFL2-AS1 can promote CRC cell proliferation *in vitro*.

3.3 IGFL2-AS1 positively regulated CA9 expression in CRC

The previous experiments confirmed that IGFL2-AS1 was principally localized in the cytoplasm (Fig. 1E), suggesting that IGFL2-AS1 may have a role in the cytoplasm. To probe the molecular mechanism by which IGFL2-AS1 promotes CRC cell proliferation, we identified the gene expression profiles of IGFL2-AS1 knockdown and control group LoVo cells by RNA sequencing analysis. Hierarchical clustering analysis results revealed that the mRNA levels between two these groups were clearly distinguishable (Fig. 4A). As

shown in the volcano plot (Fig. 4B), the IGFL2-AS1 knockdown cell population had 39 down-regulated mRNAs and 44 up-regulated mRNAs compared to the control cells (|log2 fold change|>1, *p*-value < 0.05). We then examined the expression levels of nine down-regulated mRNAs that may be associated with malignant progression and poor prognosis in CRC by qRT-PCR in LoVo cells. We found that *CA9* was the most drastically reduced gene in IGFL2-AS1 knockdown LoVo cells (Fig. 4C). In view of this phenomenon, we hypothesized that IGFL2-AS1 may have an expression and functional relationship with CA9.

To test this hypothesis, qRT-PCR and western blotting were used to assess the effect of IGFL2-AS1 on CA9 expression in HT29 and LoVo cells. The results illustrated that IGFL2-AS1 knockdown considerably reduced the mRNA and protein levels of CA9, which were significantly increased after IGFL2-AS1 overexpression (Fig. 4D, E). Subsequently, we found that the mRNA and protein levels of CA9 in five CRC cell lines were markedly increased than those in the normal colon epithelial cell line NCM460 (Fig. 4F). In addition, IHC staining was performed to evaluate the protein expression of CA9 in CRC tissues and non-tumor tissues, and the results showed that CA9 was up-regulated in tumor tissues (Fig. 4G). Similarly, from a sample analysis of the GEPIA online database (http://gepia2.cancer-pku.cn), we observed that CA9 expression was remarkably higher in CRC tissues than in normal tissues (Fig. 4H). The above results indicate that CA9 is highly expressed in CRC and positively regulated by IGFL2-AS1.

3.4 CA9 was required for IGFL2-AS1 to enhance CRC cell growth *in vitro*

As previously described, CA9 is regulated by IGFL2-AS1 and is an important prognostic marker for CRC.[19, 20] We postulate that the regulatory role of IGFL2-AS1 on CA9 expression is the reason for its promotive effect on CRC cell proliferation. To this end, we co-transfected the overexpressing CA9 vector, oeCA9, and the IGFL2-AS1 knockdown vector. Transfection efficiency was verified by qRT-PCR (Fig.S1). As speculated, the CCK-8 assay demonstrated that the CA9 overexpression enhanced the cell viability of HT29 and LoVo cells compared to controls (Fig. 5A). Similarly, EdU and colony formation assays were employed to confirm that the CA9 overexpression promoted cell proliferation (Fig. 5B–D).

Interestingly, although the absence of IGFL2-AS1 clearly impairs HT29 and LoVo cell viability, when the overexpressing CA9 vector was co-transfected with shIGFL2-AS1#1, the inhibition of CRC cell viability by IGFL2-AS1 knockdown was blocked as CA9 level increased (Fig. 5A). Similarly, EdU and colony formation assays showed that IGFL2-AS1 knockdown reversed the promotive effect of CA9 overexpression on CRC cell proliferation (Fig. 5B–D). These data indicate that CA9 is an integral factor for IGFL2-AS1 to play a pro-proliferative role in CRC.

3.5 IGFL2-AS1 upregulated CA9 expression by inhibiting HIF-1α proteolysis

Given that previous studies have confirmed that HIF-1α can bind to the upstream promoter immediately adjacent to the CA9 transcription initiation site, it may be the main transcriptional regulator of CA9.[18, 21] To explore the molecular mechanism underlying the regulation of CA9 by IGFL2-AS1, we speculated that

IGFL2-AS1 might affect HIF-1α expression in CRC cells. Western blotting was performed to test this hypothesis. The results showed that in HT29 and LoVo cells, the HIF-1α protein level was decreased in the IGFL2-AS1 knockdown groups and increased in the IGFL2-AS1 overexpression groups (Fig. 6A). Furthermore, the promotion of CA9 expression by IGFL2-AS1 overexpression was suppressed after HIF-1α knockdown in LoVo cells (Fig. 6B). These data show that HIF-1α may be involved in mediating the regulation of CA9 expression by IGFL2-AS1.

To further clarify the manner in which IGFL2-AS1 affects HIF-1α, we examined the mRNA expression of HIF-1α in knockdown and overexpressing IGFL2-AS1 cells using qRT-PCR. The results indicated no significant changes in the mRNA level of HIF-1α (Fig.S2), which was consistent with the result of RNA sequencing analysis, suggesting that IGFL2-AS1 may primarily affect the post-transcriptional regulation of HIF-1α. Under normoxic conditions, prolyl-hydroxylated HIF-1α can bind to the tumor suppressor protein von Hippel-Lindau (VHL) and is recognized by E3 ubiquitinated protein ligase for proteasomal degradation.[22, 23] Therefore, to validate the effect of the proteasome system on the HIF-1α expression level in CRC cells, we treated HT29 and LoVo cells separately for a period of time with specific concentrations of MG132 (Selleck, USA), a proteasome inhibitor. Results of western blotting indicated that HIF-1α protein content accumulated over time (Fig. 6C), suggesting that MG132 could effectively prevent the degradation of HIF-1α by the ubiquitin-proteasome system in CRC cells. Subsequently, CRC cells transfected with sh-nc, shIGFL2-AS1#1, pCDH, and oe IGFL2-AS1 were incubated with the same concentration of MG132 for 6 h, and western blotting was used to measure the change in HIF-1α protein level. Interestingly, we found that cells in the MG132-treated groups had significantly higher HIF-1α levels than those in the non-MG132-treated groups. Furthermore, MG132-induced HIF-1α accumulation was more pronounced in cells overexpressing IGFL2-AS1, while MG132 induced less HIF-1α accumulation in IGFL2-AS1 knockdown cells compared to the respective control groups (Fig. 6D). This suggests that IGFL2-AS1 can positively regulate HIF-1α expression by inhibiting the degradation by the proteasome system. In addition, the protein synthesis inhibitor cycloheximide (CHX, MCE, Shanghai, China) was employed to treat LoVo cells with stable IGFL2-AS1 knockdown or overexpression for a period of time. Results of western blotting indicated that IGFL2-AS1 knockdown accelerated the degradation of HIF-1α, whereas IGFL2-AS1 overexpression slowed down the degradation of HIF-1α protein (Fig. 6E). Collectively, these results demonstrate that IGFL2-AS1 may affect the proteolysis pathway of HIF-1α, and may increase the expression of its downstream gene *CA9* by inhibiting the degradation of HIF-1α.

3.6 IGFL2-AS1 accelerated CRC tumor growth *in vivo* via the HIF-1α/CA9 pathway

As discussed above, we demonstrated that IGFL2-AS1 can promote CRC cell proliferation *in vitro* by regulating CA9 expression. Further, a xenograft tumor model of nude mice was established to verify whether IGFL2-AS1 could accelerate tumor progression *in vivo.* LoVo cells with stable knockdown or overexpression of IGFL2-AS1 and control cells were injected subcutaneously into the right axilla of nude mice (three nude mice in each group). From day 7, the tumor size was measured every 4 days until the nude mice were sacrificed by cervical dislocation, and the tumors were harvested on day 27 (Fig. 7A, B).

As expected, slower tumor growth, smaller tumor volume, and lighter tumor weight were observed in mice in the shIGFL2-AS1#1 group than those in the sh-nc group. Similarly, compared to the control group, the tumor volume, weight, and growth rate of mice in the oe IGFL2-AS1 group were considerably higher (Fig. 7C). This evidence illustrates that IGFL2-AS1 can indeed promote CRC cell proliferation *in vivo.*

In addition, western blotting and IHC staining were utilized to detect the protein levels of HIF-1α and CA9 in tumor tissues from the nude mice in each group. The results of western blotting and IHC were consistent, in which IGFL2-AS1 knockdown in nude mouse tumor tissues reduced the HIF-1α and CA9 expression, whereas IGFL2-AS1 overexpression had the opposite results (Fig. 7D, E). Unsurprisingly, IHC staining indicated that the proliferation marker Ki67 decreased with IGFL2-AS1 knockdown, but increased in the tumor tissues of nude mice overexpressing IGFL2-AS1 (Fig. 7E). Taken together, these results confirm that IGFL2-AS1 can maintain CRC tumor growth through the HIF-1α/CA9 pathway *in vivo*.

4 Discussion

The high relapse and metastasis rates of CRC lead to poor outcomes and low long-term survival.[24] In the face of limited treatment options for advanced CRC, it is crucial to clarify the molecular mechanisms behind CRC occurrence and development.[3, 4] The next-generation sequencing technology has made it possible to identify the specific expression patterns of non-coding RNAs in various tumors, including CRC, and the possibility that lncRNAs could become novel biomarkers and therapeutic targets for CRC.[25, 26]

Based on the microarray analysis of CRC clinicopathological samples downloaded from TCGA database, we found that the lncRNA IGFL2-AS1 was drastically upregulated in CRC tissues (Table S3). Likewise, qRT-PCR confirmed that IGFL2-AS1 showed a significant overexpression trend in CRC tissues and cell lines compared to paired adjacent non-tumor tissues and normal colon epithelial cell lines. This gives us reason to speculate that IGFL2-AS1 may play an active biological role in the pathophysiology of CRC. Unsurprisingly, IGFL2-AS1 knockdown considerably reduced the viability of CRC cells, turning them into less proliferative cells both *in vivo* and *in vitro*. Conversely, CRC cells stably overexpressing IGFL2-AS1 had a greater proliferative capacity than controls. These conclusions are consistent with the phenomenon observed in previous study,[14] and further complement the results of experiments *in vivo*, providing more valuable evidence for the idea that *IGFL2-AS1* may be an oncogene in CRC.

Based on the mechanistic basis provided by the functional experiments, transcriptome sequencing analysis was utilized to explore the downstream genes of IGFL2-AS1. We validated the gene with the most sharply reduced mRNA level, *CA9*, in the IGFL2-AS1 knockdown cell population. In a variety of solid tumors, including CRC (19, 20), bladder cancer,[27] non-small cell lung cancer,[28] triple-negative breast cancer,[29] and pancreatic cancer,[30] CA9 has been widely confirmed as an oncogenic factor and diagnostic molecular marker. In the present study, we demonstrated that IGFL2-AS1 could positively regulate CA9 expression *in vitro* and *in vivo* and promote CRC development by upregulating CA9. CA9, which has a catalytic domain facing outside the cell membrane, is an enzyme that plays a central role in tumor pH regulation, and it catalyzes the balance between H^+, CO_2, and HCO_3^- inside and outside the cell.[31] Since

the accumulation of lactate resulting from increased glycolytic activity in the tumor microenvironment often activates the transmembrane transporters such as CA9,[32] the CA9 expression level may be considered a marker of tumor malignancy. In addition, CA9 can also promote the transport activity of the monocarboxylic transporter (MCT) through non-catalytic interactions, which can mediate the release of large amounts of lactate and protons from highly glycolytic tumor cells.[33, 34] The regulatory effect of CA9 on the acid-base balance of the tumor microenvironment may be the key to its tumor-promoting effect under the influence of IGFL2-AS1 in CRC.

As it is well established, the promoter of *CA9* is transactivated under various stimuli that activate HIF-1α.[21] Activation of the CA9 promoter is hardly seen in the absence of HIF-1α because the transcriptional activity of CA9 depends on the tight regulation of the hypoxia-responsive element (HRE) containing the HIF-binding site (HBS) close to transcription start site; therefore, HIF-1α is the most pivotal transcription factor of CA9.[18] Interestingly, we observed that the expression pattern of IGFL2-AS1 and HIF-1α was consistent in CRC cells. By knocking down HIF-1α in cells overexpressing IGFL2-AS1, we found that CA9 expression was decreased, as compared with that in the treatment group overexpressing IGFL2-AS1 alone. Moreover, IGFL2-AS1 could upregulate the HIF-1α expression level by inhibiting its ubiquitinated proteasomal degradation. This validates the hypothesis that the regulation of CA9 by IGFL2-AS1 is mediated by HIF-1α. Nonetheless, there are some limitations in this study. On the one hand, all experimental data were obtained under normoxic conditions, so it is unclear whether the effect of IGFL2-AS1 on the HIF-1α/CA9 pathway also exists under hypoxic conditions. On the other hand, it is not clear whether the ways in which IGFL2-AS1 affects HIF-1α degradation are direct or indirect.

HIF is a heterodimeric complex composed of the O_2-reactive functional subunit α and the stable structural subunit β, and its activity is mainly controlled by the stabilization of the α subunit (HIF-1α, HIF-2α, or HIF-3α).[35] When oxygen is abundant, the HIF-1α protein is translated but rapidly degraded. The main mechanism involves, as mentioned above, the degradation of HIF-1α modified by specific prolyl hydroxylase (PHD) by VHL via the ubiquitin-proteasome system.[36] Several mechanisms have also been proposed to explain the degradation pathway of HIF-1α. For example, the receptor of activated protein kinase C (RACK1) can compete with heat shock protein 90 (HSP90) for binding to the PAS-A domain of HIF-1α, thereby accelerating the O_2/PHD/VHL independent proteolysis of HIF-1α.[37] Activation of p53 has also been shown to accelerate proteasome-dependent HIF-1α degradation and downregulate CA9.[38] We have noted that the proteolytic mechanism of HIF-1α is complex, and the specific mode of action of IGFL2-AS1 on HIF-1α could be further researched. Furthermore, due to elevated oncogenic signaling in tumor cells, HIF-1α expression can also be regulated in an oxygen-independent manner, including effects on its mRNA transcription and translation.[35] This can result in high HIF-1α expression levels even under normoxic conditions. According to previous reports, treatment with insulin-like growth factor 1 (IGF1) can induce the protein synthesis of HIF-1α in cells.[39] The IGFL family has a similar protein structure and expression pattern to the IGF family,[40] and previous reports have confirmed that IGFL2-AS1 could promote IGFL1 expression in tumor cells.[11] Therefore, although our data suggest that IGFL2-AS1 may

primarily affect the post-transcriptional regulatory pathway of HIF-1α, whether it also acts on the protein synthesis of HIF-1α through IGFL1 in CRC needs further investigation.

In conclusion, we demonstrated that the lncRNA IGFL2-AS1 often has a tendency towards overexpression in CRC, and its expression level is an important factor affecting CRC cell proliferation. Inhibition of HIF-1α degradation by IGFL2-AS1 results in the upregulation of CA9, which then leads to the promotion of CRC growth both *in vivo* and *in vitro* (Fig. 8). Consequently, as an oncogenic factor in CRC, IGFL2-AS1 is expected to become a new valuable therapeutic target and prognostic indicator for CRC.

Declarations

Conflict of Interest

The authors have no conflict of interest.

Consent for publication

Not applicable.

Competing interests

The authors declare that they have no competing interests.

Funding Information

This study was supported by Natural Science Foundation of Chongqing, China (cstc2019jcyj-msxmX0054) and Science and Technology Planning Project of Yuzhong District of Chongqing City (20210115).

Ethics Statements

- Approval of the research protocol by an Institutional Reviewer Board: This study was conducted in accordance with the principles embodied in the Declaration of Helsinki. The experimental protocol involving human tissues for this study was approved by the Ethics Committee of the First Affiliated Hospital of Chongqing Medical University.

- Informed consent: Written informed consent was obtained from each human tissue provider.

- Animal studies: The animal experiment protocol of this study was authorized by the Animal Experiment Ethics Committee of Chongqing Medical University.

Author Contributions

MQ and ZX completed the study design. WY and QW collected clinical tissue samples. MQ and QL carried out all experiments. MQ analyzed the experimental data and wrote the manuscript. ZX reviewed the

manuscript. All authors contributed to the article and approved the submitted version.

Availability of data and materials

Not applicable.

Acknowledgments

The authors thank Editage (www.editage.cn) for English language editing.

References

1. Sung H, Ferlay J, Siegel RL, et al. Global Cancer Statistics 2020: GLOBOCAN Estimates of Incidence and Mortality Worldwide for 36 Cancers in 185 Countries. CA Cancer J Clin. **71**, 209-249(2021)
2. Kennedy RD, Bylesjo M, Kerr P, et al. Development and independent validation of a prognostic assay for stage II colon cancer using formalin-fixed paraffin-embedded tissue. J Clin Oncol. **29**, 4620-6 (2011)
3. Coppedè F, Lopomo A, Spisni R, Migliore L. Genetic and epigenetic biomarkers for diagnosis, prognosis and treatment of colorectal cancer. World J Gastroenterol. **20**, 943-56 (2014)
4. Markowitz SD, Bertagnolli MM. Molecular origins of cancer: Molecular basis of colorectal cancer. N Engl J Med. **361**, 2449-60 (2009)
5. Djebali S, Davis CA, Merkel A, et al. Landscape of transcription in human cells. Nature. **489**, 101-8 (2012)
6. Rinn JL, Chang HY. Genome regulation by long noncoding RNAs. Annu Rev Biochem. **81**, 145-66(2012)
7. Sánchez Y, Huarte M. Long non-coding RNAs: challenges for diagnosis and therapies. Nucleic Acid Ther. **23**, 15-20(2013)
8. Wu H, Qin W, Lu S, et al. Long noncoding RNA ZFAS1 promoting small nucleolar RNA-mediated 2'-O-methylation via NOP58 recruitment in colorectal cancer. Mol Cancer. **19**, 95 (2020)
9. Silva-Fisher JM, Dang HX, White NM, et al. Long non-coding RNA RAMS11 promotes metastatic colorectal cancer progression. Nat Commun. **11**, 2156 (2020)
10. Zhao R, Wang S, Tan L, Li H, Liu J, Zhang S. IGFL2-AS1 facilitates tongue squamous cell carcinoma progression via Wnt/β-catenin signaling pathway. Oral Dis (2021). doi: 10.1111/odi.13935.
11. Wang H, Shi Y, Chen CH, et al. KLF5-induced lncRNA IGFL2-AS1 promotes basal-like breast cancer cell growth and survival by upregulating the expression of IGFL1. Cancer Lett. **515**, 49-62 (2021)
12. Ma Y, Liu Y, Pu YS, et al. LncRNA IGFL2-AS1 functions as a ceRNA in regulating ARPP19 through competitive binding to miR-802 in gastric cancer. Mol Carcinog. **59**, 311-322(2020)
13. Zhou H, Xiong Y, Peng L, Wang R, Zhang H, Fu Z. LncRNA-cCSC1 modulates cancer stem cell properties in colorectal cancer via activation of the Hedgehog signaling pathway. J Cell Biochem.

121, 2510-2524 (2020)

14. Cen X, Huang Y, Lu Z, et al. LncRNA IGFL2-AS1 Promotes the Proliferation, Migration, and Invasion of Colon Cancer Cells and is Associated with Patient Prognosis. Cancer Manag Res. **13**, 5957-5968 (2021)
15. Ames S, Andring JT, McKenna R, Becker HM. CAIX forms a transport metabolon with monocarboxylate transporters in human breast cancer cells. Oncogene. **39**, 1710-1723 (2020)
16. Pastorek J, Pastorekova S. Hypoxia-induced carbonic anhydrase IX as a target for cancer therapy: from biology to clinical use. Semin Cancer Biol. **31**, 52-64 (2015)
17. Kalinin S, Malkova A, Sharonova T, et al. Carbonic Anhydrase IX Inhibitors as Candidates for Combination Therapy of Solid Tumors. Int J Mol Sci. **22**, 13405 (2021)
18. Wykoff CC, Beasley NJ, Watson PH, et al. Hypoxia-inducible expression of tumor-associated carbonic anhydrases. Cancer Res. **60**, 7075-83 (2000)
19. Korkeila E, Talvinen K, Jaakkola PM, et al. Expression of carbonic anhydrase IX suggests poor outcome in rectal cancer. Br J Cancer. **100**, 874-80 (2009)
20. Viikilä P, Kivelä AJ, Mustonen H, et al. Carbonic anhydrase enzymes II, VII, IX and XII in colorectal carcinomas. World J Gastroenterol. **22**, 8168-77 (2016)
21. Kaluz S, Kaluzová M, Liao SY, Lerman M, Stanbridge EJ. Transcriptional control of the tumor- and hypoxia-marker carbonic anhydrase 9: A one transcription factor (HIF-1) show? Biochim Biophys Acta. **1795**, 162-72 (2009)
22. Huang LE, Gu J, Schau M, Bunn HF. Regulation of hypoxia-inducible factor 1alpha is mediated by an O2-dependent degradation domain via the ubiquitin-proteasome pathway. Proc Natl Acad Sci U S A. **95**, 7987-92 (1998)
23. Maxwell PH, Pugh CW, Ratcliffe PJ. Insights into the role of the von Hippel-Lindau gene product. A key player in hypoxic regulation. Exp Nephrol. **9**, 235-40 (2001)
24. Kuipers EJ, Grady WM, Lieberman D, et al. Colorectal cancer. Nat Rev Dis Primers. **1**, 15065 (2015)
25. Shah MY, Ferrajoli A, Sood AK, Lopez-Berestein G, Calin GA. microRNA Therapeutics in Cancer - An Emerging Concept. EBioMedicine. **12**, 34-42 (2016)
26. Adams BD, Parsons C, Walker L, Zhang WC, Slack FJ. Targeting noncoding RNAs in disease. J Clin Invest. **127**, 761-771 (2017)
27. Wen J, Yang T, Mallouk N, et al. Urinary Exosomal CA9 mRNA as a Novel Liquid Biopsy for Molecular Diagnosis of Bladder Cancer. Int J Nanomedicine. **16**, 4805-4811 (2021)
28. Giatromanolaki A, Harris AL, Banham AH, Contrafouris CA, Koukourakis MI. Carbonic anhydrase 9 (CA9) expression in non-small-cell lung cancer: correlation with regulatory FOXP3+T-cell tumour stroma infiltration. Br J Cancer. **122**, 1205-1210 (2020)
29. da Motta LL, Ledaki I, Purshouse K, et al. The BET inhibitor JQ1 selectively impairs tumour response to hypoxia and downregulates CA9 and angiogenesis in triple negative breast cancer. Oncogene. **36**, 122-132 (2017)

30. Logsdon DP, Grimard M, Luo M, et al. Regulation of HIF1α under Hypoxia by APE1/Ref-1 Impacts CA9 Expression: Dual Targeting in Patient-Derived 3D Pancreatic Cancer Models. Mol Cancer Ther. **15**, 2722-2732 (2016)
31. Swietach P, Hulikova A, Vaughan-Jones RD, Harris AL. New insights into the physiological role of carbonic anhydrase IX in tumour pH regulation. Oncogene. **29**, 6509-21 (2010)
32. Hanahan D, Weinberg RA. Hallmarks of cancer: the next generation. Cell. **144**, 646-74 (2011)
33. Ames S, Pastorekova S, Becker HM. The proteoglycan-like domain of carbonic anhydrase IX mediates non-catalytic facilitation of lactate transport in cancer cells. Oncotarget. **9**, 27940-27957 (2018)
34. Ames S, Andring JT, McKenna R, Becker HM. CAIX forms a transport metabolon with monocarboxylate transporters in human breast cancer cells. Oncogene. **39**, 1710-1723 (2020)
35. Keith B, Johnson RS, Simon MC. HIF1α and HIF2α: sibling rivalry in hypoxic tumour growth and progression. Nat Rev Cancer. **12**, 9-22 (2011)
36. Keith B, Simon MC. Hypoxia-inducible factors, stem cells, and cancer. Cell. **129**, 465-72 (2007)
37. Liu YV, Baek JH, Zhang H, Diez R, Cole RN, Semenza GL. RACK1 competes with HSP90 for binding to HIF-1alpha and is required for O(2)-independent and HSP90 inhibitor-induced degradation of HIF-1alpha. Mol Cell. **25**, 207-17 (2007)
38. Kaluzová M, Kaluz S, Lerman MI, Stanbridge EJ. DNA damage is a prerequisite for p53-mediated proteasomal degradation of HIF-1alpha in hypoxic cells and downregulation of the hypoxia marker carbonic anhydrase IX. Mol Cell Biol. **24**, 5757-66 (2004)
39. Fukuda R, Hirota K, Fan F, Jung YD, Ellis LM, Semenza GL. Insulin-like growth factor 1 induces hypoxia-inducible factor 1-mediated vascular endothelial growth factor expression, which is dependent on MAP kinase and phosphatidylinositol 3-kinase signaling in colon cancer cells. J Biol Chem. **277**, 38205-11 (2002)
40. Emtage P, Vatta P, Arterburn M, et al. IGFL: A secreted family with conserved cysteine residues and similarities to the IGF superfamily. *Genomics.* **88**, 513-20 (2006)

Figures

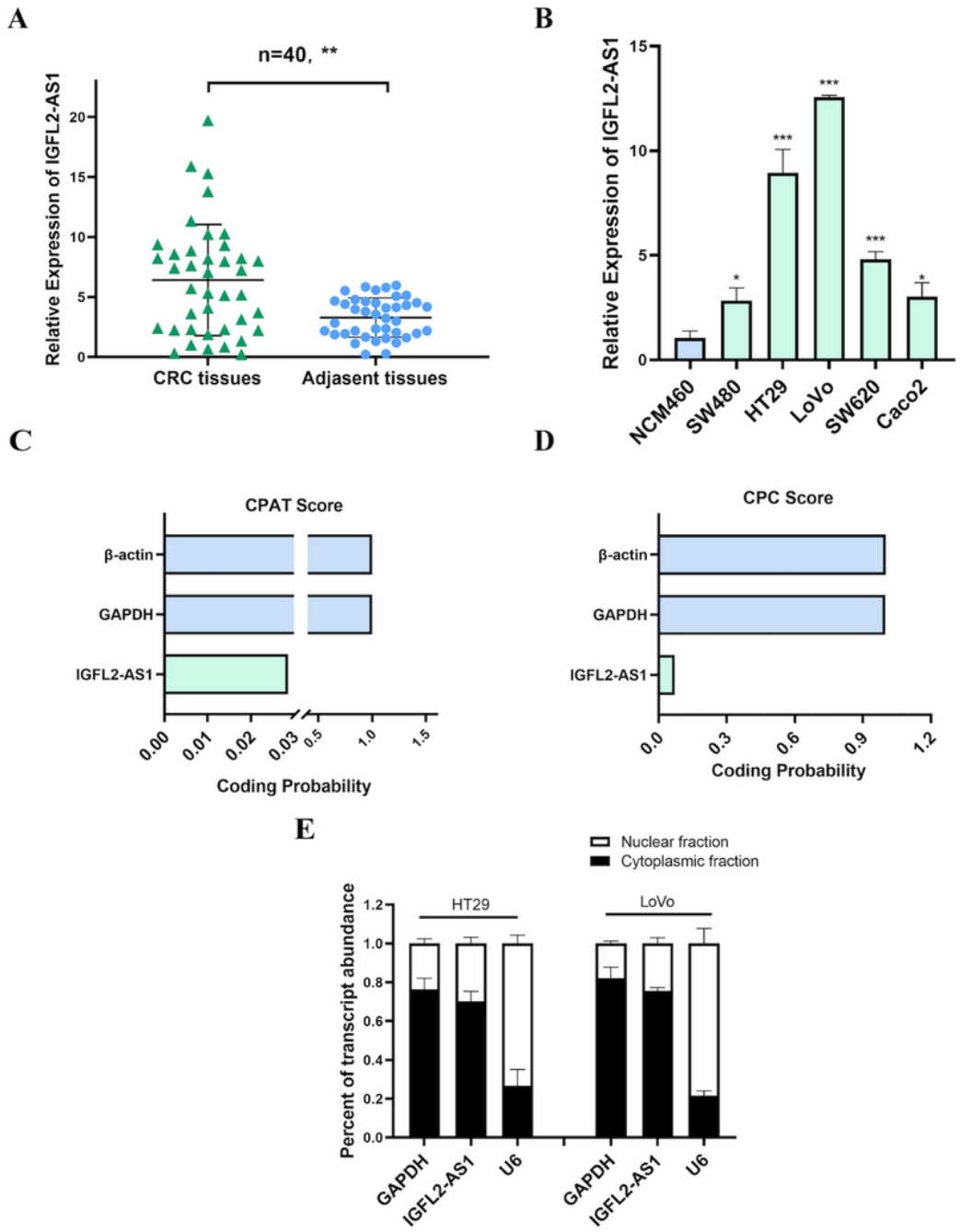

Figure 1

IGFL2-AS1 expression level in CRC. (A) IGFL2-AS1 expression in 40 pairs of colorectal cancer tumor tissues and adjacent normal tissues. (B) IGFL2-AS1 expression in five colorectal cancer cell lines and normal colon epithelial cell lines. GAPDH was used as the internal control. (C, D) The protein coding ability of IGFL2-AS1 was detected using CPAT (C) and CPC (D). (E) The subcellular localization of IGFL2-AS1 in HT29 and LoVo cells. (*$p<0.05$, **$p<0.01$, ***$p<0.001$

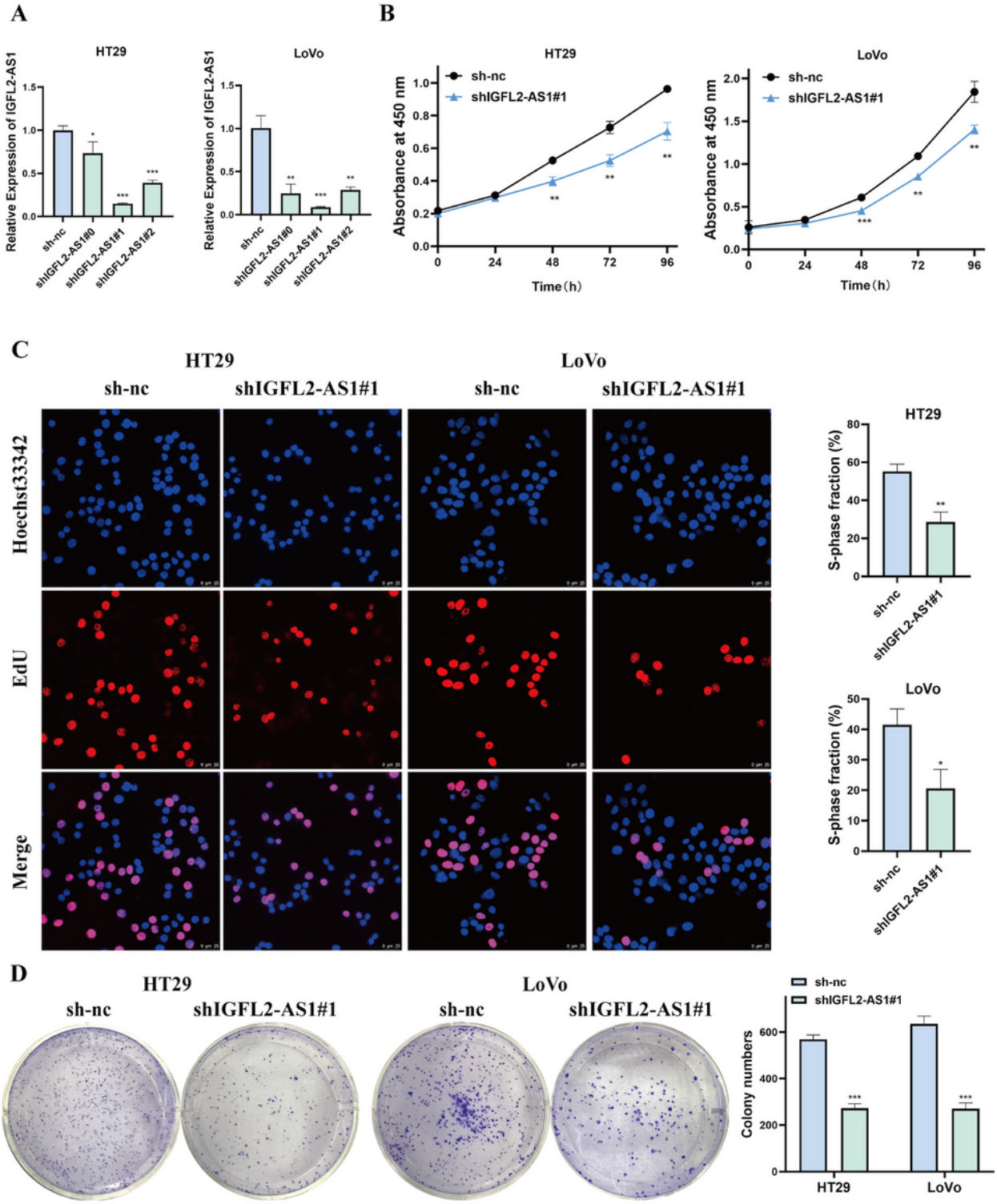

Figure 2

IGFL2-AS1 knockdown inhibits CRC cell growth *in vitro*. (A) The knockdown efficiency of IGFL2-AS1 in HT29 and LoVo cells was verified by qRT-PCR. (B) CCK-8 assay was utilized to detect the effect of IGFL2-AS1 knockdown on the viability of HT29 and LoVo cells. (C, D) Proliferation ability of HT29 and LoVo cells in the IGFL2-AS1 knockdown group and negative control group was analyzed by EdU assay (C) and clone formation assay (D). (magnification, 400×; scale bar, 25 μm; **p<0.05, **p<0.01, ***p<0.001*)

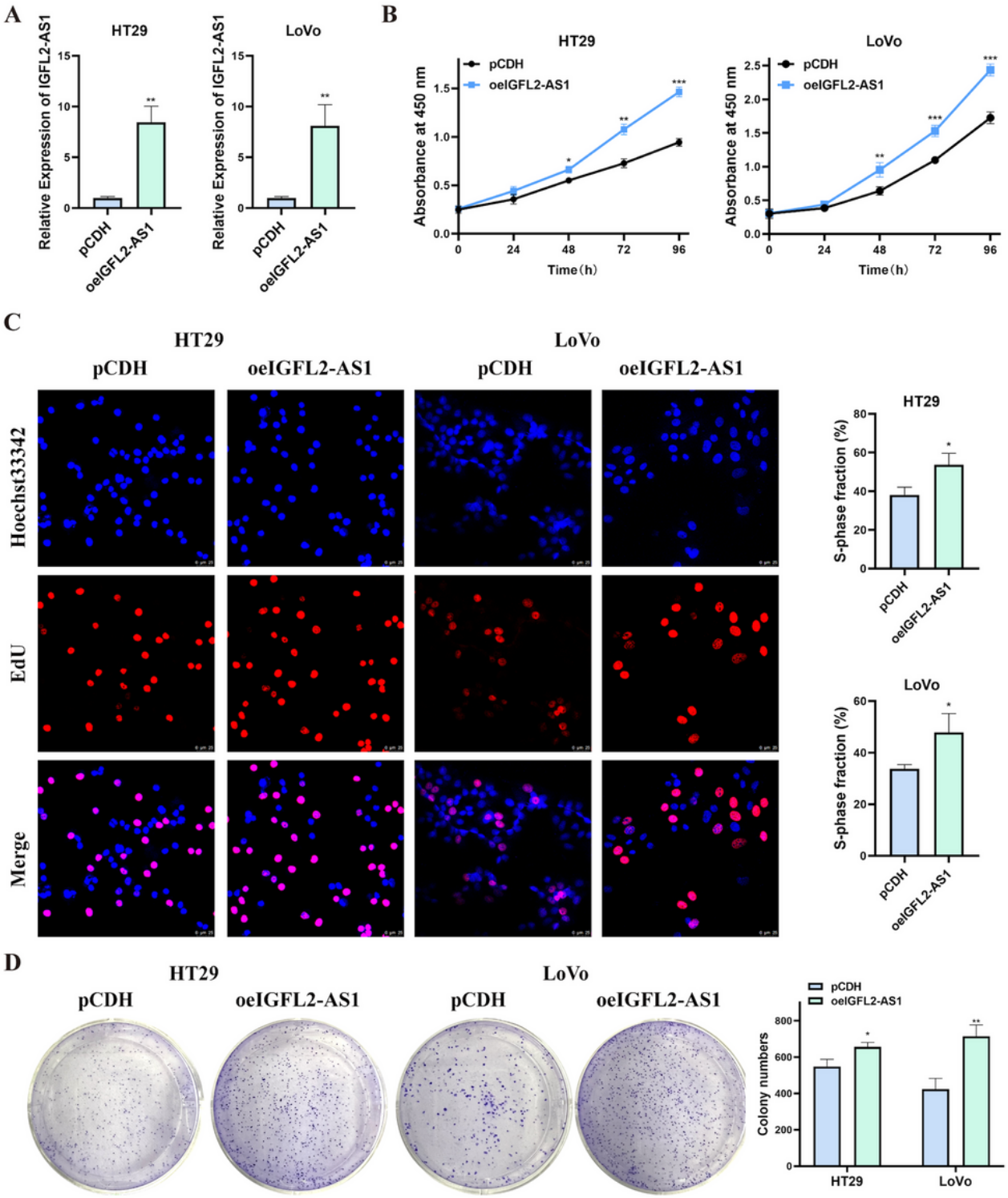

Figure 3

IGFL2-AS1 overexpression promotes CRC cell proliferation *in vitro*. (A) qRT-PCR was employed to assess the overexpression efficiency in CRC cells. (B) The difference in cell viability of CRC cells in the IGFL2-AS1 overexpressing group and control group was measured by CCK-8 assay. (C, D) The effect of IGFL2-AS1

overexpression on CRC cell proliferation was detected by EdU assay (C) and clone formation assay (D). (magnification, 400×; scale bar, 25 μm; **p<0.05, **p<0.01, ***p<0.001*)

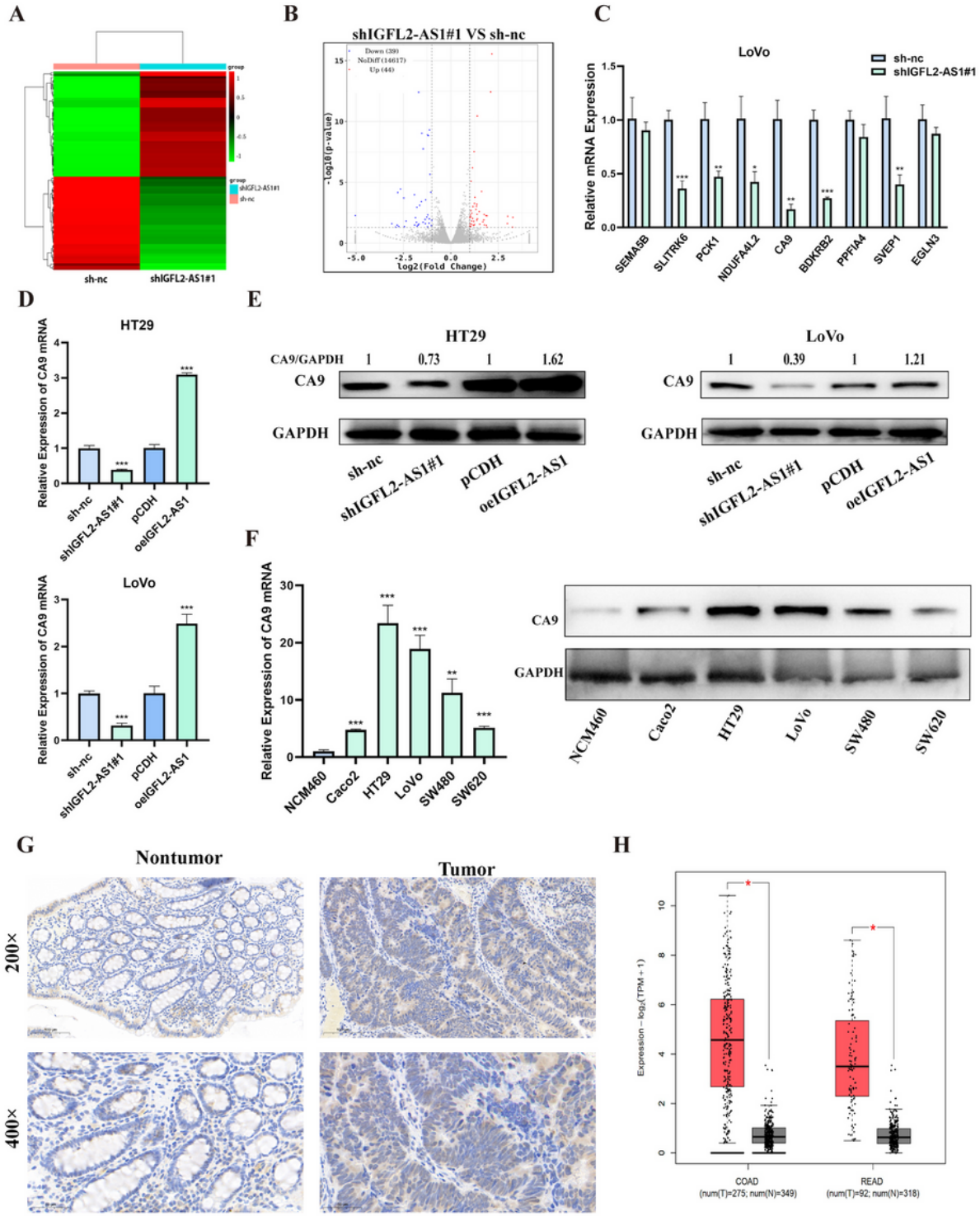

Figure 4

IGFL2-AS1 positively regulates CA9 expression in CRC. (A, B) Differential gene heat map (A) and volcano map (B) of negative control and IGFL2-AS1 knockdown LoVo cell populations. Upregulation is shown as red, and downregulation is shown as green. (C) mRNA levels of 9 downregulated genes in IGFL2-AS1 knockdown LoVo cells were measured by qRT-PCR. (D, E) qRT-PCR and western blotting were utilized to detect mRNA (D) and protein (E) levels of CA9 in HT29 and LoVo cells that overexpress or knockdown IGFL2-AS1. (F) Immunohistochemistry was performed to assess the protein level of CA9 in CRC tumor tissue and adjacent non-tumor tissue. (G) CA9 expression in TCGA-derived specimen datasets in the GEPIA database. (magnification, 200× and 400×; scale bar, 100 μm and 50 μm; *$p<0.05$, **$p<0.01$, ***$p<0.001$*)

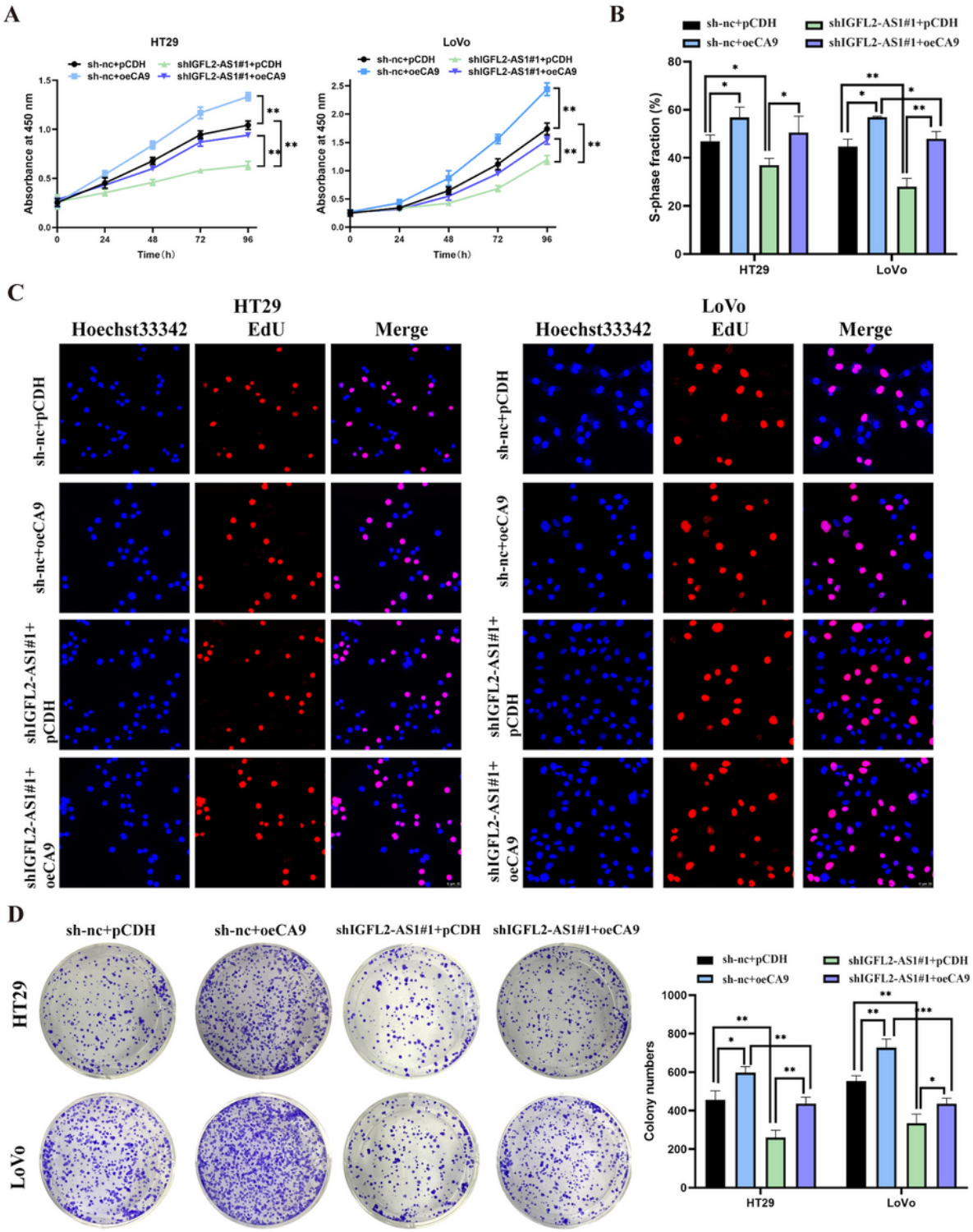

Figure 5

CA9 is required for IGFL2-AS1 to enhance CRC cell growth *in vitro*. (A) The effect of CA9 regulated by IGFL2-AS1 on CRC cell viability was detected by CCK-8 assay. (B, C) The quantitative results and images of the EdU assay showing that IGFL2-AS1 regulates CRC cell proliferation through CA9. (D) The effect of CA9 overexpression and IGFL2-AS1 knockdown co-transfection on CRC cell proliferation was examined using a colony formation assay. (magnification, 400×; scale bar, 25 μm; **p<0.05, **p<0.01, ***p<0.001*)

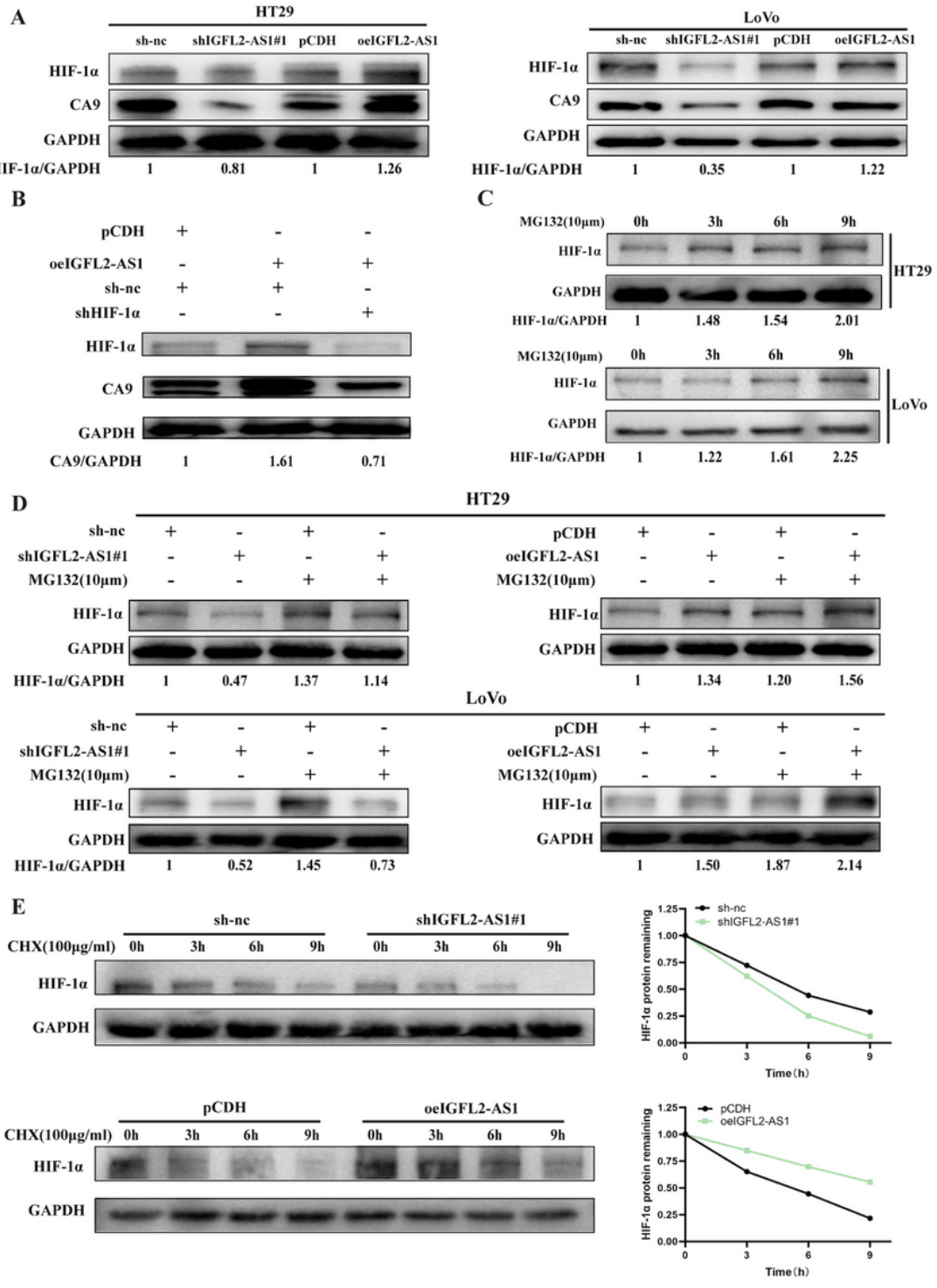

Figure 6

IGFL2-AS1 upregulates CA9 expression by inhibiting HIF-1α proteolysis. (A) Western blotting was used to assess the HIF-1α and CA9 expression levels in CRC cells with IGFL2-AS1 knockdown and overexpression. (B) The effect of HIF-1α knockdown on the increase in CA9 protein level by IGFL2-AS1

overexpression. (C) The protein levels of HIF-1α after HT29 and LoVo cells were treated with MG132 (10 μM) for 0, 3, 6, and 9 h were measured by western blotting. (D) CRC cells were transfected with sh IGFL2-AS1#1, oe IGFL2-AS1, or negative control, and treated with or without MG132 (10 μM) for 6 h. The protein levels of HIF-1α were detected by western blotting. (E) CRC cells in IGFL2-AS1 knockdown and overexpression groups were treated with CHX (100 μg/ml) for 0, 3, 6, and 9 h, and western blotting was performed to measure the HIF-1α expression levels

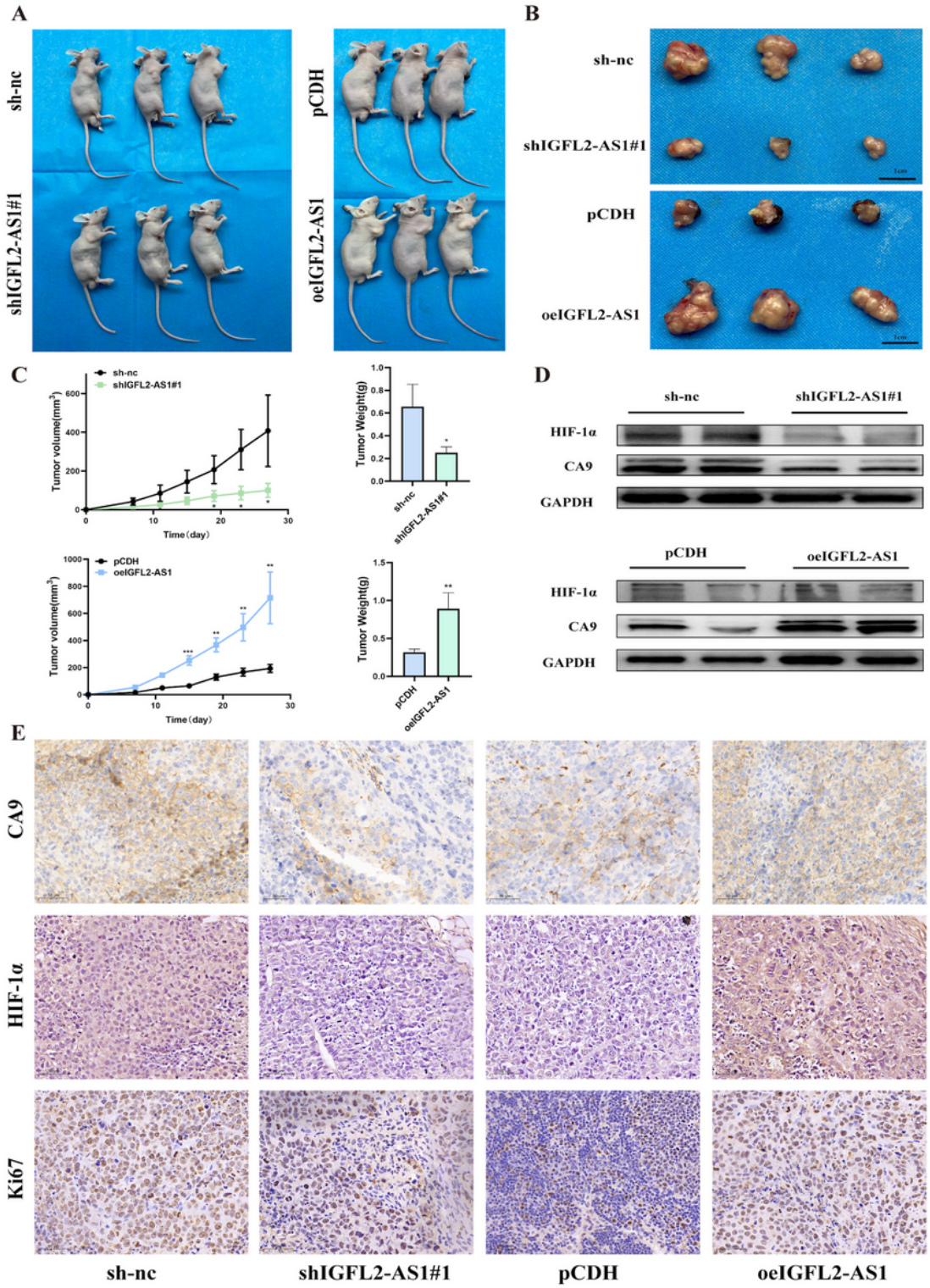

Figure 7

IGFL2-AS1 accelerates CRC tumor growth *in vivo.* (A, B) All mice were sacrificed on day 27 after injection, and tumors were harvested and photographed. (C) The histogram of tumor weight and the tumor growth curve based on measured tumor volume. (D) Western blotting was performed to verify the protein levels of HIF-1α and CA9 in the tumors of nude mice in each group. Two samples were taken from each group.

(E) Immunohistochemical staining of HIF-1α, CA9, and Ki67 in xenograft tumors. (scale bar, 1 cm; *$p<0.05$, **$p<0.01$, ***$p<0.001$)

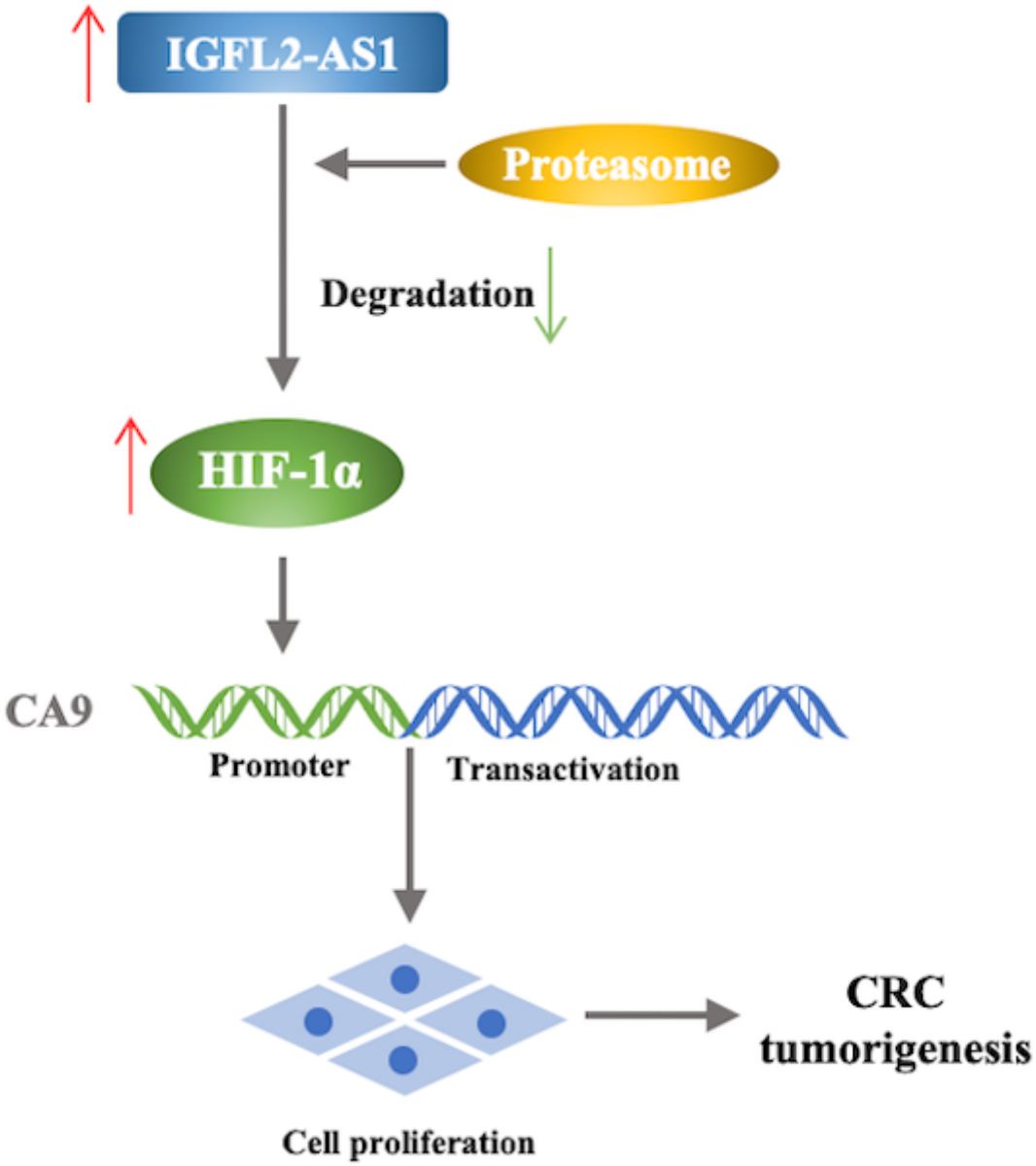

Figure 8

The schematic illustration of a model for IGFL2-AS1 to promote tumor growth in CRC. IGFL2-AS1 is up-regulated in CRC and may inhibit the proteasomal degradation of HIF-1α, which could increase HIF-1α expression and its downstream gene CA9, thereby promoting CRC cell proliferation

Supplementary Files

This is a list of supplementary files associated with this preprint. Click to download.

- SupplementaryMaterial.docx